Lawrence Berkeley National Laboratory
LBL Publications

Title
Studies of N{sub 2}0 adsorption and decomposition on Fe-ZSM-5

Permalink
https://escholarship.org/uc/item/9xs9p249

Journal
Journal of Catalysis, 209(1)

Authors
Wood, Benjamin R.
Reimer, Jeffrey A.
Bell, Alexis T.

Publication Date
2002-03-08

Studies of N$_2$O Adsorption and Decomposition on Fe-ZSM-5

Benjamin R. Wood, Jeffrey A. Reimer, and Alexis T. Bell*

Chemical Sciences Division
Lawrence Berkeley National Laboratory
and
Department of Chemical Engineering
University of California
Berkeley, CA 94720-1462

*Author to whom correspondence should be sent: bell@cchem.berkeley.edu

Abstract

The interactions of N_2O with H-ZSM-5 and Fe-ZSM-5 have been investigated using infrared spectroscopy and temperature-programmed reaction. Fe-ZSM-5 samples with Fe/Al ratios of 0.17 and 0.33 were prepared by solid-state exchange. It was determined that most of the iron in the samples of Fe-ZSM-5 is in the form of isolated cations, which have exchanged with Brønsted acid H^+ in H-ZSM-5. The infrared spectrum of N_2O adsorbed on H-ZSM-5 at 298 K exhibits bands at 2226 and 1308 cm^{-1} associated with vibrations of the N-N and N-O bonds, respectively. The positions of these bands relative to those seen in the gas phase suggest that N_2O adsorbs through the nitrogen end of the molecule. The heat of N_2O adsorption in H-ZSM-5 is estimated to be 5 kcal/mol. In the case of Fe-ZSM-5, additional infrared bands are observed at 2282 and 1344 cm^{-1} due to the interactions of N_2O with the iron cations. Here too, the directions of the shifts in the vibrational features relative to those for gas-phase N_2O suggest that the molecule adsorbs through its nitrogen end. The heat of adsorption of N_2O on the Fe sites is estimated to be 16 kcal/mol. The extent of N_2O adsorption on Fe depends on the oxidation state of Fe. The degree of N_2O adsorption is higher following pretreatment of the sample in He or CO at 773 K, than following pretreatment in O_2 or N_2O at the same temperature. Temperature-programmed decomposition of N_2O was performed on the Fe-ZSM-5 samples and revealed that N_2O decomposes stoichiometrically to N_2 and O_2. A higher activity was observed if the catalysts were pretreated in He than if they were pretreated in N_2O. For the He-pretreated samples, the activation energy for N_2O decomposition was estimated to be 42 kcal/mol and the preexponential factor of the rate coefficient for this

process was found to increase with Fe/Al ratio. This trend was attributed to the

increasing autoreducibility of Fe^{3+} cations to Fe^{2+} cations with increasing Fe/Al ratio.

Introduction

Iron-exchanged ZSM-5 is a potentially useful material for the removal of N_2O from industrial waste streams. At low temperatures, Fe-ZSM-5 can be used to remove low concentrations of N_2O by adsorption.[1] At temperatures above 573 K, it is an active catalyst for the decomposition of N_2O to N_2 and O_2.[2,3,4,5,6] It has been demonstrated that N_2O-pretreated Fe-ZSM-5 will react with methane to form methoxide species, which can subsequently be hydrolyzed to produce methanol.[3,7,8,9,10,11] Fe-ZSM-5 has also been shown to be active for the oxidation of benzene to phenol using N_2O as the oxidant.[3,9] For these reasons, there is an active interest in determining the states of iron in Fe-ZSM-5 and their interaction with N_2O.

Lobree et al. have reported that at loadings below Fe/Al = 0.56, Fe^{3+} cations exchange on a one to one basis with Brønsted acid protons, but at higher Fe/Al ratios, small particles of Fe_2O_3 particles appear to form.[12] Sachtler and coworkers have reported similar findings.[13] Evidence for iron oxide clusters and diferric μ-oxygen-bridged cations have been reported in recent EXAFS studies. Joyner and Stockenhuber have concluded from such studies that the distribution of iron in Fe-ZSM-5 is strongly dependent on the manner of iron exchange and pretreatment. Depending on these factors, they see evidence of isolated iron cations, large clusters of Fe_3O_4, as well as Fe_4O_4 nanoclusters.[14] On the other hand, Marturano et al. have shown using EXAFS that the distribution of iron in Fe-ZSM-5 is strongly dependent on the structure of the parent ZSM-5 with evidence for both diferric μ-oxo-bridged clusters and Fe_2O_3 particles.[15] Battison et al. have also provided EXAFS data supporting the existence of diferric oxo clusters.[16]

The present work was undertaken to examine the mode and strength of N_2O adsorption on Fe-ZSM-5 and the activity of this catalyst for N_2O decomposition. Samples of Fe-ZSM-5 were prepared with Fe loadings significantly lower than Fe/Al = 1, in order to assure that all of the exchanged Fe was present as isolated cations. The roles of Fe/Al ratio and oxidative versus reductive pretreatment were also examined.

Experimental

H-ZSM-5 was prepared by mixing 30 g of Na-ZSM-5 (Alsi-Penta , Si/Al = 25) with 360 ml of a 1 M solution of NH_4NO_3 (Fisher brand in de-ionized water), at room temperature for 12 h. The resulting product was filtered and the recovered zeolite was washed with 700 ml of de-ionized water. This procedure was repeated two additional times and the wet product was then dried in an oven at 383 K for 2 h. The resulting NH_4-ZSM-5 was calcined in air to produce H-ZSM-5. Calcination was carried out in a quartz reactor into which 1.45 g of NH_4-ZSM-5 was placed. The flow rate of air was set to 50 cm^3/min. The reactor was then heated from 298 K to 823 K over a period of 4 h, maintained at 823 K for 8 h, and then cooled to room temperature.

Fe-ZSM-5 was produced from H-ZSM-5 by solid-state exchange using the following procedure. Four grams of NH_4-ZSM-5 were calcined as described above. After 8 h at 823 K, the air flow was stopped and the reactor was purged at 823 K for 1 h with a 50 cm^3/min flow of helium. The reactor was then cooled to room temperature in helium and sealed. The sealed reactor was placed into a glove box, where it was opened and the resulting H-ZSM-5 was removed and ground with an appropriate amount of $FeCl_3$ using a mortar and pestle. This mixture was returned to the quartz reactor, resealed, and

removed from the glove box. The reactor was subsequently heated from 298 K to 583 K

over a period of 5 h under 50 cm^3/min of He, and maintained at 583 K for an additional 2

h. The reactor was then cooled to room temperature and the resulting Fe-ZSM-5 was

removed from the reactor and ground once again with a mortar and pestle. Two Fe-ZSM-

5 samples with differing Fe/Al ratios were produced for this study. These samples are

designated as Fe-ZSM-5(0.17) and Fe-ZSM-5(0.33), where the quantity in parenthesis

denotes the atomic Fe/Al ratio in the final products. After the introduction of Fe, each

sample was washed repeatedly with de-ionized water to remove Cl$^-$ and the final product

was dried in an oven at 383 K for 1 h. Elemental analyses of the samples (Galbraith

Laboratories) used in this work are shown in Table 1.

Infrared spectra were recorded using a Nicolet Nexus 670 FT-IR equipped with an

MCT-A detector. Measurements were made at a resolution of 4 cm^{-1} with a total of 64

scans per spectrum. Total gas flow rates for all experiments were 60 ml/min. Samples

were pressed into 30 mg self-supporting pellets, and subsequently placed into an IR cell

equipped with either BaF$_2$ or CaF$_2$ IR windows.[17] Prior to initiating experiments with a

new pellet, the cell temperature was raised to 773 K at 1 K/min in flowing He and then

held at the final temperature for 3 h.

Prior to recording a spectrum of the hydroxyl-stretching region, the sample was

pretreated in helium at 773 K. The temperature of the cell was then decreased to 523 K

and a spectrum of the pellet was recorded. The cell was then cooled to 298 K where

experiments were performed in which N$_2$O in helium was adsorbed on the samples. In a

separate experiment a spectrum was also taken of the empty cell at 523 K under helium

using the same procedure. This background was subtracted from the spectrum of the sample to remove any absorbance due to the CaF_2 windows.

Experiments were performed in which various concentrations of N_2O were adsorbed on samples at 298 K while measuring IR absorption. In these experiments, the sample was pretreated for 2 h at 773 K in helium, 3.00% N_2O in helium, 10.3% O_2 in helium, or 4.22% CO in helium. The sample was then cooled to 298 K and a background spectrum of the sample in helium was recorded. The sample was then exposed to various concentrations of N_2O in helium and spectra were recorded after 23 min. The background spectrum of the sample in helium was then subtracted to obtain a spectrum consisting of only absorbances due to adsorbed species on the zeolite.

A number of experiments were performed in which samples were heated from 298 K to 768 K in 5,000 ppm N_2O in helium while measuring IR absorption. The first step in these experiments was a N_2O pretreatment, as described above. The sample was then cooled to 298 K in helium. Once at 298 K, the sample was exposed to the gas mixture for 5 minutes, at which point the ramp in temperature to 768 K was begun. The ramp rate was 1 K/min. In a separate experiment a set of background spectra were taken of the sample in helium while heating from 298 K to 768 K. These background spectra were subtracted from those taken under 5,000 ppm N_2O to obtain spectra consisting of only absorbances do to adsorbed species on the zeolite.

Temperature-programmed decomposition of N_2O was carried out with a sample (100 mg) placed in a quartz micro-reactor. The effluent from the reactor was monitored using a UTI model 100C Mass Spectrometer. Prior to initiating a temperature-programmed decomposition experiment, the sample was heated in flowing helium (60 ml/min) from

298 K to 773 K over a period of 1 h. Upon reaching 773 K, the sample was held in

helium for an additional 3 h and then cooled to 298 K. Next, the sample was exposed to

15,000 ppm N_2O in helium (total flow rate = 60 ml/min) for 8 min at 298 K. The

temperature was then ramped at 5 K/min from 298 K to 773 K. Following this procedure

the sample was cooled to 298 K, and the entire procedure was then repeated after

pretreating the sample in 3.00% N_2O.

Results

Lobree et al.[12] have demonstrated that for similarly prepared Fe-ZSM-5, iron cations

exchange on a one-for-one basis with Brønsted acid protons up to an Fe/Al ratio of 0.56.

To establish the level of proton exchange for the Fe-ZSM-5 samples used in this study, a

spectrum of the hydroxyl-stretching region of Fe-ZSM-5(0.33) was recorded at 523 K

and compared to that of H-ZSM-5 recorded at the same temperature. As seen in Figure 1,

bands are observed at 3740 cm^{-1} and 3601 cm^{-1}. The band at 3740 cm^{-1} is assigned to O-

H stretching vibrations of silanol groups while the band at 3601 cm^{-1} is assigned to O-H

stretching vibrations of Brønsted acid groups.[12,14,18,19] The intensity of the Brønsted acid

hydroxyl group decreases with the introduction of iron, indicating that iron cations have

replaced H^+ at the charge-exchange sites. By taking the ratio of the intensity of the band

at 3601 cm^{-1} for Fe-ZSM-5(0.33) to that for H-ZSM-5, it is determined that Fe cations

have exchanged with about 28% of the protons. This corresponds closely to the amounts

obtained via elemental analysis, 33%, confirming that most of the iron introduced into the

zeolite is present as isolated iron cations at the charge-exchange sites.

Infrared spectra were acquired after exposing H-ZSM-5, Fe-ZSM-5(0.17), and Fe-ZSM-5(0.33) to N_2O. Prior to N_2O exposure, each sample was pretreated in helium at 773 K and then cooled to 298 K. A background spectrum was then recorded in helium. Next, the sample was exposed to 5,000 ppm N_2O in helium (total flow rate = 60 cm^3/min) for 23 min before recording the spectrum. The resulting spectra are displayed in Figure 2. N_2O interacting with H-ZSM-5 displays a strong band at 2226 cm^{-1}, and a weak band at 1308 cm^{-1}. For Fe-ZSM-5(0.17) and Fe-ZSM-5(0.33), two additional bands are observed, one at 2282 cm^{-1} and the other 1344 cm^{-1}. The intensities of these bands increase with increasing iron loading, indicating that these features are attributable to the interaction of N_2O with Fe cations.

Gas-phase N_2O exhibits two primary bands, an N-N stretching vibration at 2224 cm^{-1}, and an N-O stretching vibration at 1286 cm^{-1}. [20,21,22] Consequently, the bands at 2282 cm^{-1} and 2226 cm^{-1} are assigned to N-N stretching vibrations while the bands at 1344 cm^{-1} and 1308 cm^{-1} are assigned to N-O stretching vibrations. The absence of any roto-vibrational bands, suggests that the bands at 2226 cm^{-1} and 1308 cm^{-1} on H-ZSM-5 and the additional bands at 2282 cm^{-1} and 1344 cm^{-1} on Fe-ZSM-5 are not due to gas-phase N_2O.[23] It is notable that the bands at 1344 cm^{-1} and 1308 cm^{-1} are much less intense than the bands at 2282 cm^{-1} and 2226 cm^{-1}. Bands near 1300 cm^{-1} are expected to be suppressed owing to the intense adsorption of the IR windows. Joyner et al. report evidence of the appearance of adsorbed nitric oxide as well nitrogen dioxide or nitrate ions up adsorption of N_2O on Fe-ZSM-5 at room temperature.[24] In the present study, no evidence of these species was observed.

To better understand the origin of the bands at 2226 cm^{-1} and 1308 cm^{-1} for N$_2$O interacting with H-ZSM-5, a series of spectra were recorded as a function of N$_2$O concentration. The results of these experiments are shown in Figure 3. With increasing N$_2$O concentration, the intensities of the bands at 2226 cm^{-1} and 1308 cm^{-1} increase montonically. These changes are accompanied by a decrease in the intensity of the negative band at 3610 cm^{-1} and an increase in intensity of a new band appearing at 3445 cm^{-1}. As discussed below, the changes in these features provide direct evidence for the interactions of N$_2$O with Brønsted acid sites in H-ZSM-5. A similar set of experiments were also performed on Fe-ZSM-5(0.17) (Figure 4). The results are identical to those for H-ZSM-5, except for the additional bands due to N$_2$O adsorbed on Fe observed at 2282 cm^{-1} and 1344 cm^{-1}. It is observed that the intensities of these bands do not increase with increasing gas-phase N$_2$O beyond that observed for 2,000 ppm N$_2$O, indicating that the Fe sites are completely saturated with N$_2$O at 2,000 ppm N$_2$O.

Experiments were preformed to determine the effect of the oxidation state of iron on the adsorption of N$_2$O. For these experiments, Fe-ZSM-5(0.33) was subjected to various pretreatments at 773 K and then cooled to 298 K. A background spectrum was recorded in helium and the sample was then exposed for 23 min to 5,000 ppm N$_2$O in helium (total flow rate = 60 cm^3/min). The sample was first pretreated at 773 K for 2 h in helium, after which the spectrum of adsorbed N$_2$O was recorded. The sample was then reduced in CO at 773 K for 2 h, after which the spectrum of adsorbed N$_2$O was recorded again. The sample was then oxidized in O$_2$ and a spectrum of N$_2$O adsorbed on the oxidized sample was recorded. A second cycle of CO reduction and N$_2$O adsorption was carried out. Finally, the sample was oxidized in N$_2$O and a spectrum of adsorbed N$_2$O recorded. The

spectrum of adsorbed N_2O recorded after each pretreatment is displayed in Fig. 5. The intensity of the band at 2282 cm^{-1}, assigned to N_2O adsorbed on iron sites, remains the same after the He pretreatment and following the first CO reduction. A significant reduction in the intensity of the band occurs following oxidation in O_2. However, the band intensity is fully recovered if the sample is again reduced in CO. Following the N_2O pretreatment, the intensity of this band again decreases. Thus, oxidation in either O_2 or N_2O result in a decrease in intensity of the band at 2282 cm^{-1}, while reduction in CO results in the restoration of the band intensity to the level observed following helium pretreatment.

In situ infrared experiments were performed to investigate the effect of heating on the desorption and decomposition of N_2O adsorbed on H-ZSM-5 and Fe-ZSM-5. Figure 6 shows that the spectrum recorded at 298 K for N_2O adsorbed on H-ZSM-5 is identical to that presented in Figure 2. With increasing temperature, the intensity of the band at 2226 cm^{-1} decreases rapidly and the feature at 2238 cm^{-1}, which was previously observed as shoulder, becomes more prominent. A new band at 2210 cm^{-1} also becomes evident at higher temperatures. The intensities of the features at 2238 cm^{-1} and 2210 cm^{-1} decrease together as the temperature is raised above 398 K. Although a definitive assignment of these bands cannot be made, we propose that they may be due to N_2O adsorbed on Al^{3+} cations located at either defect sites in the zeolite framework or extra-framework structures, such as AlO^+.

Figure 7 shows a series of spectra recorded during an experiment in which Fe-ZSM-5(0.33) was heated in 5,000 ppm of N_2O. The features associated with N_2O interacting with the Brønsted acid sites and Al^{3+} cations behave in the same way as shown for H-

ZSM-5 in Figure 6. The feature at 2282 cm^{-1}, associated with N_2O adsorbed on Fe

cations, decreases less with increasing temperature than the feature at 2226 cm^{-1} (N_2O

interacting with Brønsted acid sites), indicating a stronger binding of N_2O to the Fe

cations than Brønsted acid sites.

The data in Figures 6 and 7 were used to determine the heat of N_2O adsorption on

protons and iron sites in H-ZSM-5 and Fe-ZSM-5 respectively. In the case of Fe-ZSM-5,

Fig. 7 shows that at 298 K the iron sites are saturated by N_2O when the partial pressure of

N_2O is 2,000 ppm. The heat of adsorption could then be determined from the slope of a

plot of $\ln[A/(A_o-A)]$ versus $1/T$, where A and A_o are the integrated absorbance for the

band at 2282 cm^{-1} at a particular coverage of the iron sites and at saturation coverage,

respectively. Since saturation coverage of the more weakly adsorbing protons could not

be achieved at 298 K and an N_2O concentration of 30,000 ppm, the extent of occupancy

of the Bronsted acid sites was determined by measuring the attenuation in the integrated

absorbance of the band at 3601 cm^{-1} for bridging hydroxyl groups. The heats of N_2O

adsorption on iron and protons are found to be 16 kcal/mol and 5 kcal/mol, respectively.

Temperature-programmed decomposition experiments were carried out in order to

investigate the effects of iron loading and catalyst pretreatment on the rate of N_2O

decomposition. Prior to each experiment the sample was pretreated in helium and then

ramped in temperature from 298 K to 773 K in 15,000 ppm N_2O in He flowing at 60

cm^3/min. The gas-phase composition was monitored by mass spectroscopy. This

experiment was repeated after the sample had been pretreated in 15,000 ppm N_2O at 773

K. The results of these experiments for H-ZSM-5, Fe-ZSM-5(0.17), and Fe-ZSM-5(0.33)

are shown in Figures 8, 9, and 10 respectively. For the experiment with H-ZSM-5, it is

seen that there is no appreciable decomposition of N_2O until a temperature of 691 K. Above this temperature, N_2O begins to decompose, forming a stoichiometric amount of N_2 and O_2 (N_2 is not shown). In the absence of the zeolite no reaction products were observed below 773K; therefore, the activity displayed by H-ZSM-5 may be due to the small amount of Fe present in the zeolite (Fe/Al = 0.1). For Fe-ZSM-5(0.17), following the helium pretreatment, the concentration of N_2O begins to decrease at 628 K and continue to decrease up to 773 K. The disappearance of N_2O is accompanied by the formation of a stoichiometric amount of N_2 and O_2. The same behavior is observed following N_2O pretreatment. For Fe-ZSM-5(0.33), however, the results differ. Following He pretreatment, N_2O begins to decompose at a 573 K, accompanied by the formation of stoichiometric amounts of N_2 and O_2. The rate of N_2O decomposition increases with temperature up to 676 K, at which point the rate of N_2O decomposition and O_2 formation level off. These rates begin to increase again at 695 K. By 773 K, almost all of the N_2O has decomposed. Following N_2O pretreatment, N_2O again begins to decompose above 573 K and stoichiometric amounts of N_2 and O_2 are generated. It is observed, however, that the rate of N_2 and O_2 formation is less than that following He pretreatment up to a temperature of 714 K. Above 714 K the rates of N_2O decomposition are almost the same for the two different pretreatments. In addition, the step seen in the decomposition rate following N_2O pretreatment is far less pronounced than that observed for following helium pretreatment.

Discussion

Recent investigations using CH_4 as a probe molecule have shown that upon adsorption, the IR spectrum of methane is perturbed relative to that seen for gas phase CH_4.[25] This is accompanied by a decrease in intensity of the band at 3610 cm^{-1} for the bridging hydroxyl group and the appearance of a band at 3445 cm^{-1} for the O-H vibrations of bridging hydroxyl groups interacting with the adsorbed CH_4. Similar results have also been observed for CO and N_2 interacting with [Ga]-H-ZSM-5.[18] The spectra presented in Figures 3 show similar behavior for N_2O adsorbed on H-ZSM-5. The adsorption of N_2O on H-ZSM-5 produces bands at 2226 and 1308 cm^{-1} attributable to adsorbed N_2O. The band at 3601 cm^{-1} associated with Brønsted acid protons decreases in intensity and a new band appears at 3445 cm^{-1}. These latter observations provide direct evidence for the interaction of N_2O with Brønsted acid sites in H-ZSM-5.

The adsorption of N_2O on iron cations in Fe-ZSM-5 results in the appearance of infrared bands at 2282 cm^{-1} and 1344 cm^{-1}, as shown in Figure 2. Both bands are blue shifted relative to gas-phase N_2O by a larger amount than the bands due to N_2O interacting with H-ZSM-5. The larger shift is consistent with the stronger binding of N_2O to Fe cations than protons (i.e., 16 kcal/mol versus 5 kcal/mol). A similar pattern between the strength of probe molecule adsorption and the magnitude of the shift in the positions of infrared bands relative to those seen in the gas phase has been observed for methane adsorbed in metal-exchanged H-ZSM-5.[26]

Having established that N_2O adsorption occurs on both isolated iron cations and Brønsted acidic protons in Fe-ZSM-5, it is desirable to determine whether these interactions take place through the oxygen or the nitrogen end of the molecule. Borello et

al.[27] have proposed that, for N_2O adsorption onto Lewis acids, the direction of the shifts in the N-N and N-O stretching bands relative to their positions in the gas phase is indicative of the mode of N_2O adsorption. Based on molecular orbital arguments, the authors suggest that if adsorption occurs through the nitrogen end of the molecule, the N-N and N-O stretching vibrations are both blue-shifted, whereas if adsorption is through the oxygen end, the N-N stretching vibration is blue-shifted and the N-O vibration is red shifted. This conclusion is supported by molecular orbital calculations conducted by Grodzicki et al. for N_2O adsorption on Ca^{2+}.[28] Ramis et al. have shown that the magnitude of the trends reported by Borello et al. become more pronounced as the Lewis acidity increases. [29] In the present study both the N-N and N-O stretching vibrations for N_2O adsorbed on iron sites are blue shifted relative to the gas phase, suggesting that N_2O adsorbs to iron through the nitrogen end. To test this hypothesis, density functional theory calculations were carried out for a 34-atom cluster used to represent the Fe cation and the associated portion of the zeolite. The cluster is centered on an Al atom in the T12 site of the MFI framework. As shown in Table 2, the calculated shifts in the vibrational frequencies of both the N-N and the N-O bonds are both positive when N_2O is assumed to be adsorbed through the nitrogen end of the molecule. However, when the adsorption of N_2O is taken to be through the oxygen end of the molecule, the N-N vibrations are shifted upscale and the N-O vibrations are shifted downscale relative to gas-phase N_2O. The experimentally observed shifts in the N-N and N-O vibrations for N_2O interacting with Brønsted acid sites in H-ZSM-5 and Fe-ZSM-5 are similar to those seen for N_2O interacting with Fe cations. This leads to the conclusion that N_2O also interacts with Brønsted acid sites through the nitrogen end of the molecule.

The data presented in Figure 5 demonstrate that the N_2O adsorption capacity of Fe in Fe-ZSM-5 depends on the mode of catalysts pretreatment. Using catalyst preparation and pretreatment procedures similar to those used in the present work, Lobree et al.[12] have shown that as-exchanged Fe is present as $Fe(OH)_2^+$. For Fe/Al < 0.19 the as-exchanged Fe^{3+} cations do not undergo extensive autoreduction ($[Fe(OH)_2]^+ \rightarrow [FeO]^+ + H_2O$); however, at higher Fe/Al ratios some of the iron cations can be autoreduced to Fe^{2+} by heating the sample in He at 773 K. Kucherov and Shelef reached an identical conclusion based on EPR studies of Fe-ZSM-5.[30] Together these findings provide a basis for interpreting the experiments shown in Figure 5 in which N_2O was adsorbed on Fe-ZSM-5(0.33) following various pretreatments. It is proposed that during He pretreatment at 773 K, a fraction of iron in the sample is autoreduced. The resulting Fe^{2+} cations adsorb N_2O, leading to the appearance of the band at 2282 cm^{-1}. Reduction of the He pretreated sample does not increase the fraction of iron in the +2 state and consequently no further increase is seen in the intensity of the band for adsorbed N_2O (see Figure 5). O_2 pretreatment results in a decrease in the intensity of the band at 2282 cm^{-1}, suggesting that oxidation of Fe^{2+} to Fe^{3+} causes a decrease in the N_2O adsorption capacity of the sample. Similar results were obtained for Fe-ZSM-5(0.17). This is surprising since Lobree et al. indicate that, for Fe/Al < 0.19, the oxidation state iron should be unaffected by the nature of the pretreatment.

The data presented in Figures 8-10 was used to calculate the apparent first order rate coefficient for N_2O decomposition over H-ZSM-5 and Fe-ZSM-5. Table 3 shows that the apparent activation energy for N_2O decomposition is virtually the same for He-pretreated H-ZSM-5 and the two samples of Fe-ZSM-5, 42±1 kcal/mol. Since H-ZSM-5 contains a

small amount of Fe (Fe/Al = 0.04), the uniformity of the activation energy suggests that the active center in all cases are iron cations. It is also likely that the active form of iron for N_2O decomposition is Fe^{2+}, since preoxidation of Fe-ZSM-5 reduces its activity (see Figs. 9 and 10). Table 3 also shows that the preexponential factor for the apparent rate coefficient increases with increasing content of iron in the catalyst. This trend is ascribed to the greater ease of autoreduction of iron with increasing Fe/Al ratio, consistent with the results reported earlier by Lobree et al.[12] The authors suggested such a trend might be associated with a change in the siting of the Fe cations with increasing Fe/Al ratio. Based on the work of Wichterlová and coworkers, they hypothesized that with increasing Fe/Al ratio, the distribution of Fe into α sites would increase and the distribution of Fe into β sites would decrease.[31] The results reported in Table 3 could be rationalized if the Fe^{3+} cations in the α sites were easier to autoreduce than those in the β sites.

A step in the decomposition rate similar to that seen in the present work for Fe-ZSM-5(0.33) (Figure 10) was also reported by Panov et al. for samples containing 0.50 wt % Fe.[3] Chen et al.[32] have observed a similar behavior from N_2O decomposition on Cu-ZSM-5. These authors suggest that the step is due to a change in the oxidation state of the copper from Cu^+ to Cu^{2+} as adsorbed oxygen is released into the gas phase. Comparison of the present results for He and N_2O pretreated Fe-ZSM-5 suggest that the observed step is also related to a change in the oxidation state of the metal cation. For both Fe-ZSM-5(0.33) and Fe-ZSM-5(0.17), the rate of N_2O decomposition decreases when the catalyst is oxidized. This trend is consistent with results reported by Sachtler et al. for Fe-ZSM-5.[4] The extent to which oxidation affects the catalyst activity increases with the extent of Fe loading. This trend is also consistent with the previous suggestion

that the fraction of Fe^{3+} capable of undergoing autoreduction to Fe^{2+} increases with increasing Fe/Al ratio.

The apparent activation energies and preexponential factors reported by Panov and co-workers are compared in Table 3 to the present results.[2] The activation energies reported by these authors as well as the preexponential factors for samples with similar Fe/Al are comparable to those reported in the present work. In the case of H-ZSM-5, both the activation energy and the preexponential factor for N_2O decomposition measured by Panov and coworkers is considerably lower than that reported in this study. This difference may be a consequence of the significantly lower Fe loading in the former case. In fact, at a Fe/Al ratio of 0.003, N_2O decomposition may be more likely to occur on extraframework AlO^+ cations than on Fe^{2+} cations.

Sachtler et al. have reported in situ IR evidence for the formation of nitro and nitrate species adsorbed on Fe-ZSM-5 after exposure of Fe-ZSM-5 to 10% N_2O in helium at 473 K, although these same bands are not observed after exposure to lower concentrations of N_2O.[4,13] They suggest that these species may be important intermediates in the decomposition mechanism for N_2O over Fe-ZSM-5 at higher N_2O concentrations. This has also been proposed by Lund et al.[5,6] In the present study, there was no evidence for any adsorbed species on Fe-ZSM-5, other then N_2O, for temperatures up to 773 K (Figure 7), indicating that, at least for the relatively low partial pressures used, nitro and nitrate species do not appear to play a role in the mechanism of N_2O decomposition.

Conclusions

N_2O adsorbed on H-ZSM-5 at 298 K exhibits infrared bands at 2226 and 1308 cm^{-1} associated with vibrations of the N-N and N-O bonds, respectively. Quantum chemical calculations indicate that the shifts in the observed bands relative to those seen in the gas phase indicate that N_2O adsorbs through the nitrogen end of the molecule. The heat of N_2O adsorption in H-ZSM-5 is estimated to be 5 kcal/mol. In the case of Fe-ZSM-5, infrared bands are observed at 2282 and 1344 cm^{-1} due to the interactions of N_2O with iron cations. Here too, the directions of the shifts in the vibrational features relative to those for gas-phase N_2O suggest that the molecule is adsorbed through its nitrogen end. The heat of adsorption of N_2O on the Fe sites is estimated to be 16 kcal/mol. The extent of N_2O adsorption on Fe is higher following sample pretreatment in He at 773 K, than following pretreatment in O_2 or N_2O at the same temperature. Temperature-programmed decomposition of N_2O performed on the Fe-ZSM-5 sample reveals that N_2O decomposes to stoichiometrically to N_2 and O_2. A higher activity was observed if the catalyst was pretreated in He than if was pretreated in N_2O. For the He-pretreated sample, the activation energy for N_2O decomposition is 42 kcal/mol and the preexponential factor of the rate coefficient for this process increases with Fe/Al ratio. The trend in the preexponential factor is attributed to the increasing ease of converting Fe^{3+} cations to Fe^{2+} cations via autoreduction ($Z[Fe(OH)_2] = Z(FeO) + H_2O$) with increasing Fe/Al ratio.

References

[1] Centi, G., Generali, P., dall'Olio, L., Perathoner, S., *Ind. Eng. Chem. Res*. **39**, 131 (2000).

[2] Panov, G. I., Sobolev, V. I., Kharitonov, A. S., *J. Mol. Catal*. **61**, 85 (1990).

[3] Panov, G. I., Uriarte, A. K., Rodkin, M. A., Sobolev, V. I.., *Catal. Today* **41**, 365 (1998).

[4] El-Malki, E. M., van Santen, R. A., Sachtler, W. M. H.., *Microporous Mater*. **35**, 235 (2000).

[5] Sang, C., Lund, C. R. F., *Catal. Lett*. **70**, 165 (2000).

[6] Sang, C., Lund, C. R. F., *Catal. Lett*. **73**, 73 (2001).

[7] Sobolev, V. I., Dubkov, K. A., Panna, O. V., Panov, G. I., *Catal. Today* **24**, 251 (1995).

[8] Panov, G. I., Sobolev, V. I., Dubkov, K. A., Parmon, V. N., Ovanesyan, N. S., Shilov, A. E., Shteinmen, A. A., *React. Kinet. Catal. Lett*. **61**, 251 (1997).

[9] Dubkov, K. A., Sobolev, V. I., Talsi, E. P., Rodkin, M. A., Watkins, N. H., Shteinman, A. A., Panov, G. I., *J. Mol. Catal. A: Chem*. **123**, 155 (1997).

[10] Knops-Gerrits, P. P., Smith, W. J., *Studies Surf. Sci. and Catal*. **130**, 3531 (2000).

[11] Knops-Gerrits, P. P., Goddard III, W. A., *J. Mol. Catal. A, Chem*. **166**, 135 (2001).

[12] Lobree, L J., Hwang, I. C., Reimer, J. A., Bell, A. T., *J. Catal*. **186**, 242 (1999).

[13] El-Malki, E. M., van Santen, R. A., Sachtler, W. M. H., *J. Catal*. **196**, 212 (2000).

[14] Joyner, R., Stockenhuber, M., *J. Phys. Chem. B*. **103**, 5963 (1999).

[15] Marturano, P., Drozdová, L., Kogelbauer, A., Prins, R., *J. Catal*. **192**, 236 (2000).

[16] Battison, A. A., Bitter, J. H., Koningsberger, D. C. *Catal. Lett*. **66**, 75 (2000).

[17] Joly, J. F., Zanier-Szyldowski, N., Colin, S., Raatz, F., Saussey, J., Lavalley, J. C. *Catal. Today* **9**, 31 (1991).

[18] Knözinger, H., Huber, S., *J. Chem. Soc., Faraday Trans*. **94**, 2047 (1998).

[19] Hadjiivanov, K., Saussey, J., Freysz, J. L., Lavalley, J. C., *Catal. Lett*. **52**, 103 (1998).

[20] Zecchina, A., Cerruti, L., Borello, E., *J. Catal*. **25**, 55 **(**1972).

[21] Nakamoto, K., "Infrared and Raman Spectra of Inorganic and Coordination Compounds", 5th ed., Wiley & Sons: New York, 1997.

[22] Lin, J., Chen, H. Y., Chen, L., Tan, K. L., Zeng, H. C., *Appl. Surf. Sci*. **103**, 307 (1996).

[23] Pouchert, C. J., "The Aldrich Library of FT-IR Spectra, Vapor Phase", 1st ed., Aldrich Chemical Company, Milwaukee, WI, 1989, Vol. 3.

[24] Grubert, G., Hudson, M. J., Joyner, R. W., Stockenhuber, M., *J. Catal*. **196**, 126 (2000).

[25] Khaliullin, R. Z., Bell, A. T., and Kazansky, V. B., *J. Phys. Chem*., in press.

[26] Kazansky, V. B., and Bell, A. T., unpublished results.

[27] Borello, E., Cerruti, L., Ghiotti, G., Guglielminotti, E., *Inorg. Chim. Acta* **6**, 45 (1972).

[28] Grodzicki, M., Zakharieva-Pencheva, O., Forster, H., *J. Mol. Struc*. **175**, 199 (1988).

[29] Ramis, G., Busca, G., Bregani, F., *Gazz. Chim. Ital*. **122**, 79 (1992).

[30] Kucherov, A. V., Shelef, M., *J. Catal*. **195**, 112 (2000).

[31] Wichterlová, B, Dedecek, J., Sobalik, Z., in "Catalysis by Unique Metal Ion Structures in Solid Matrices – From Sceince to Applications" (G. Centi, B. Wichterlová, A. T. Bell, Kluwer, Eds.), p. 31. Amsterdam, 2001.

[32] Chen, L., Chen, H. Y., Lin, J., Tan, K. L., *Surf. Interface Anal*. **28**, 115 (1999).

Figure captions

Figure 1. Infrared spectra of the hydroxyl-stretching region of (a) H-ZSM-5, and (b) Fe-ZSM-5(0.33) at 523 K following helium pretreatment.

Figure 2. Infrared spectra of 5,000 ppm N_2O adsorbed on (a) H-ZSM-5, (b) Fe-ZSM-5(0.17), and (c) Fe-ZSM-5(0.33) at 298 K following helium pretreatment.

Figure 3. Infrared spectra of (a) 30,000 ppm, (b) 10,000 ppm, (c) 7,000 ppm, and (d) 5,000 ppm N_2O adsorbed on H-ZSM-5 at 298 K following N_2O pretreatment.

Figure 4. Infrared spectra of (a) 10,000 ppm, (b) 7,000 ppm, (c) 5,000 ppm, and (d) 2,000 ppm N_2O adsorbed on Fe-ZSM-5(0.17) at 298 K following N_2O pretreatment.

Figure 5. Infrared spectra of 5,000 ppm N_2O adsorbed on Fe-ZSM-5(0.33) at 298 K following (a) He pretreatment, (b) CO pretreatment, (c) O_2 pretreatment, (d) CO pretreatment, and (e) N_2O pretreatment at 773 K.

Figure 6. Infrared spectra of 5,000 ppm N_2O adsorbed on H-ZSM-5 at (a) 298 K, (b) 348 K, (c) 398 K, (d) 448 K, (e) 498 K, and (f) 608 K following N_2O pretreatment.

Figure 7. Infrared spectra of 5,000 ppm N_2O adsorbed on Fe-ZSM-5(0.33) at (a) 298 K, (b) 348 K, (c) 378 K, (d) 398 K, (e) 448 K, (f) 498 K, and (g) 608 k following N_2O pretreatment.

Figure 8. Temperature programmed decomposition profile, (a) N_2O and (b) O_2, for 15,000 ppm N_2O over H-ZSM-5 following He pretreatment.

Figure 9. Temperature programmed decomposition profile for 15,000 ppm N_2O over Fe-ZSM-5(0.17) following He pretreatment, (a) N_2O and (b) O_2, and N_2O pretreatment, (c) N_2O and (d) O_2.

Figure 10. Temperature programmed decomposition profile for 15,000 ppm N_2O over Fe-ZSM-5(0.33) following He pretreatment, (a) N_2O and (b) O_2, and N_2O pretreatment, (c) N_2O and (d) O_2.

Table 1

Sample Elemental Analysis

Sample	Fe wt%	Fe/Al
H-ZSM-5	0.04	0.01
Fe-ZSM-5(0.17)	0.57	0.17
Fe-ZSM-5(0.33)	1.11	0.33

Table 2

Calculated Frequency Shifts for N_2O adsorbed on Fe-ZSM-5

Mode[a]	NNO-$(OFe)^+Z^-$	ONN-$(OFe)^+Z^-$
$\Delta\nu$(N-N)	+15 cm^{-1}	+49 cm^{-1}
$\Delta\nu$(N-O)	-49 cm^{-1}	+47 cm^{-1}

(a) Calculated frequency shift relative to gas-phase N_2O.

Table 3

Activation Energies and Preexponential Factors Calculated from Temperature Programmed Decomposition Experiments Following He Pretreatment

Sample[a]	Fe wt%	Activation energy (kcal/mol)	Preexponential Factor (mol N_2O/s•mol Fe•Pa N_2O)	Ref.
H-ZSM-5(0.01)	0.04	42.4	8.8×10^7	This work
Fe-ZSM-5(0.17)	0.57	42.1	2.0×10^8	This work
Fe-ZSM-5(0.33)	1.11	42.7	3.2×10^9	This work
H-ZSM-5(0.0016)	0.0028	23 ± 1.5	5.0×10^2	(2)
Fe-ZSM-5(0.033)	0.056	35 ± 4	3.1×10^7	(2)
Fe-ZSM-5(0.21)	0.35	37 ± 1.5	1.0×10^8	(2)

(a) Samples are designated as either H-ZSM-5(x) or Fe-ZSM-5(x), where x indicates the Fe/Al ratio. The Si/Al ratio is 25 in this work and 50 in the work of Panov and coworkers (2).
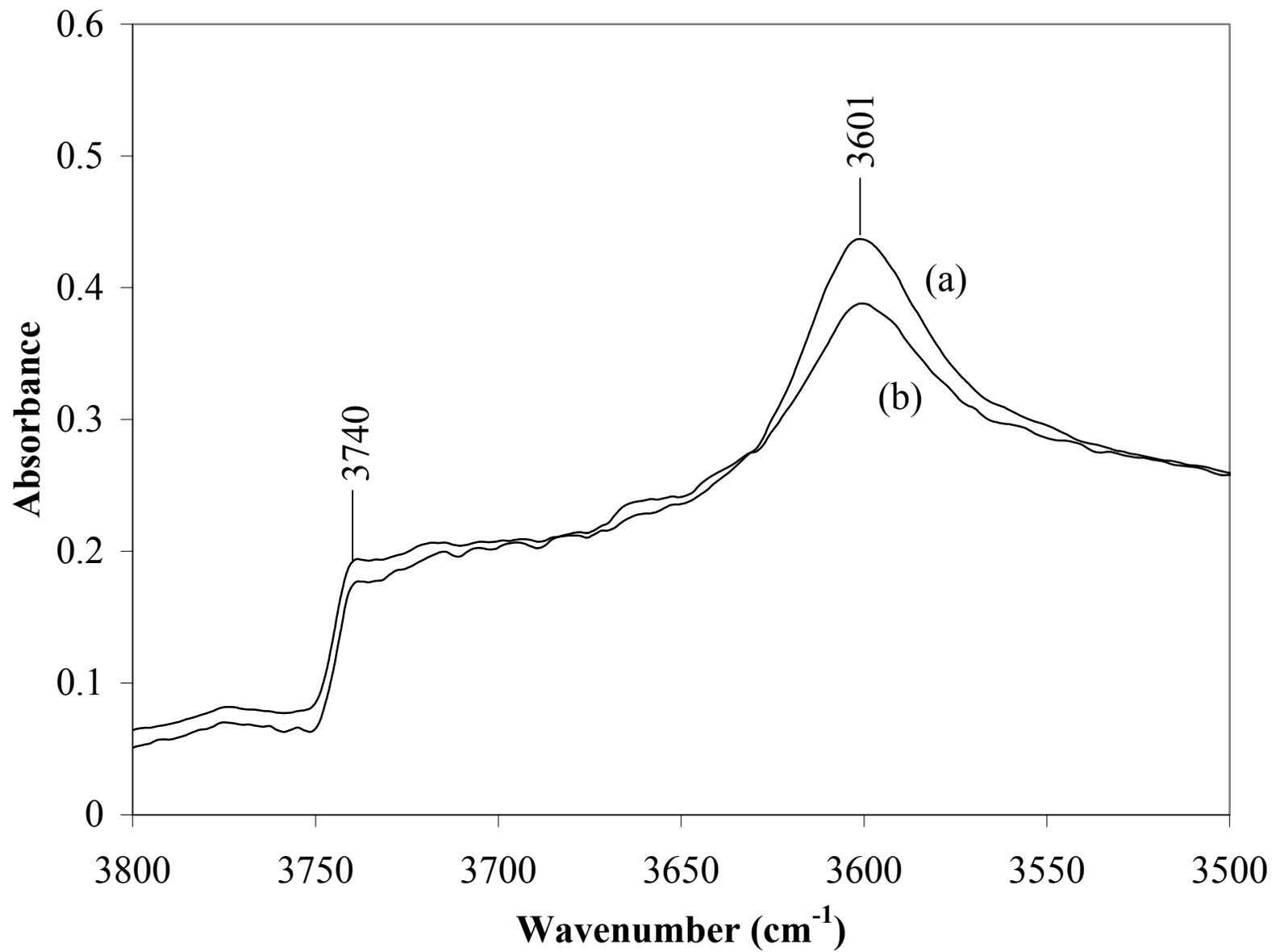
Fig. 1
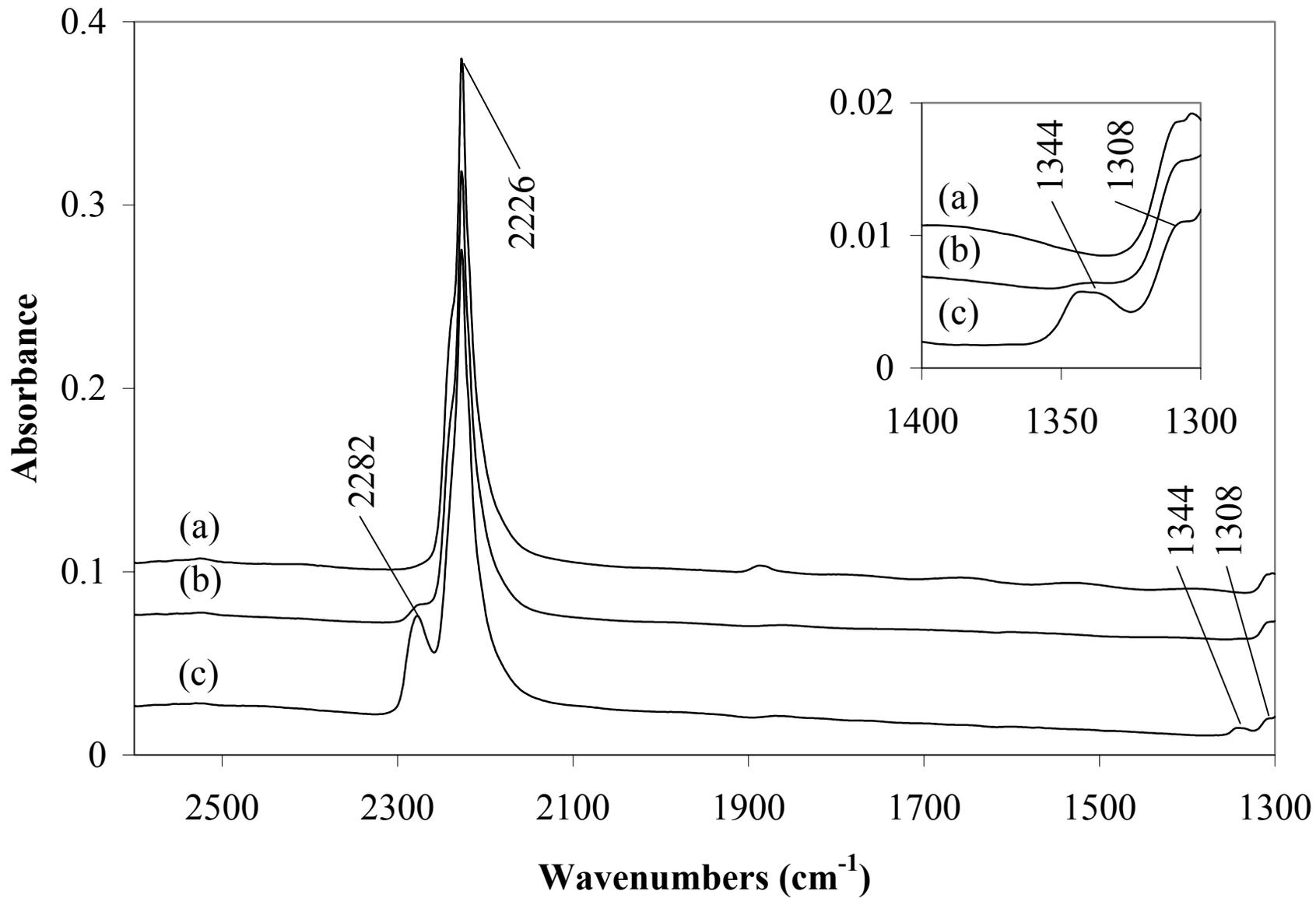
Fig. 2
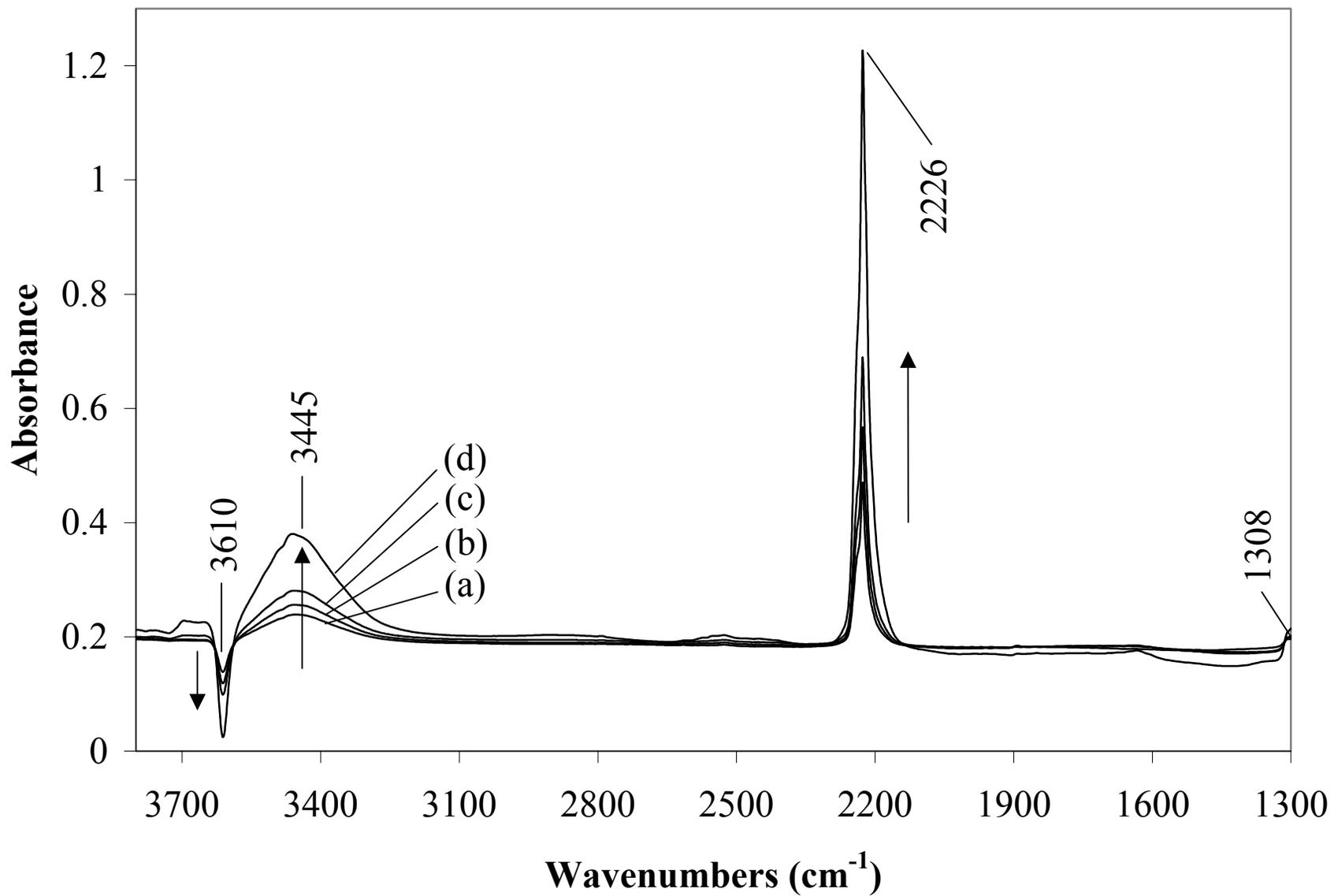
Fig. 3
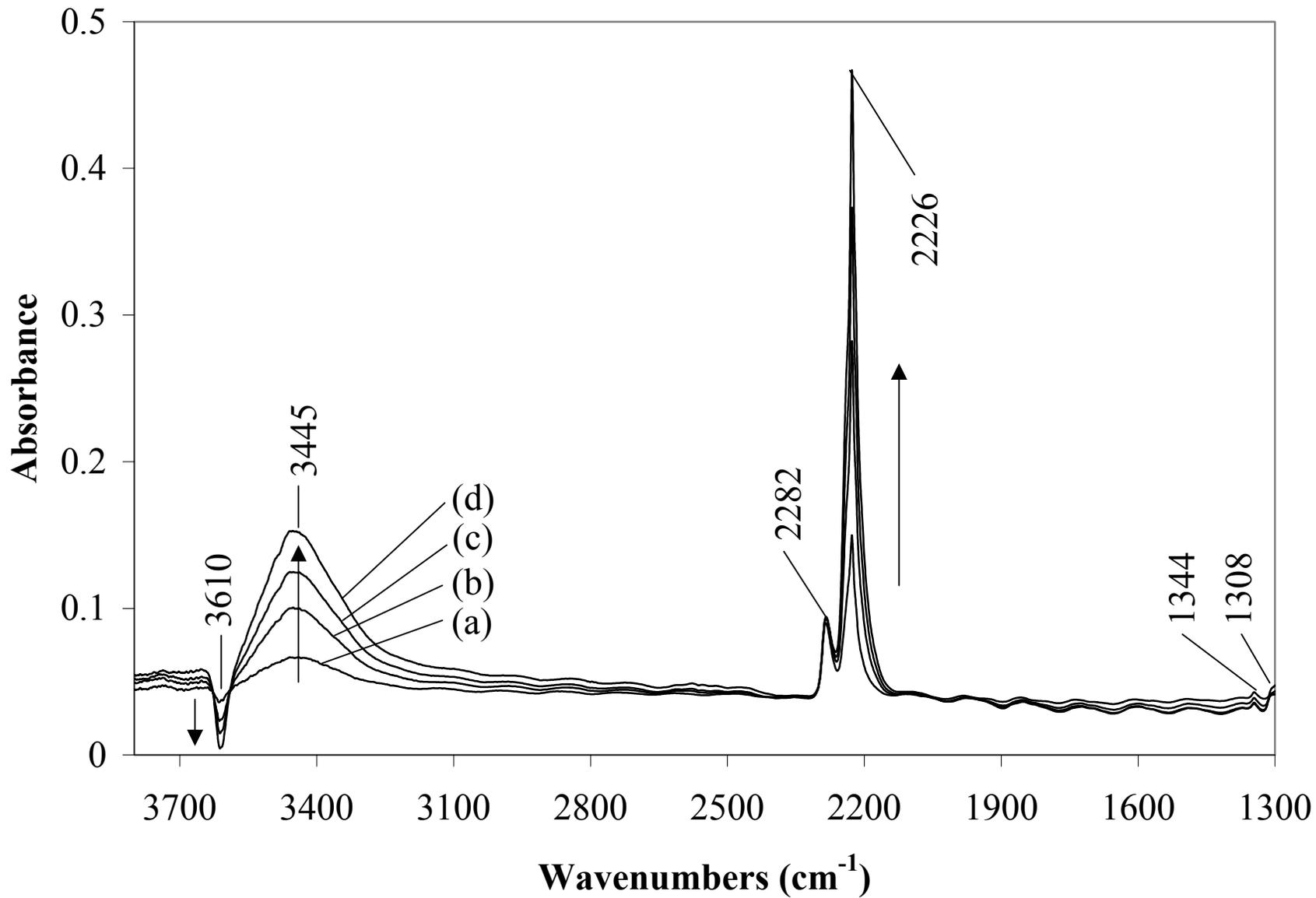
Fig. 4
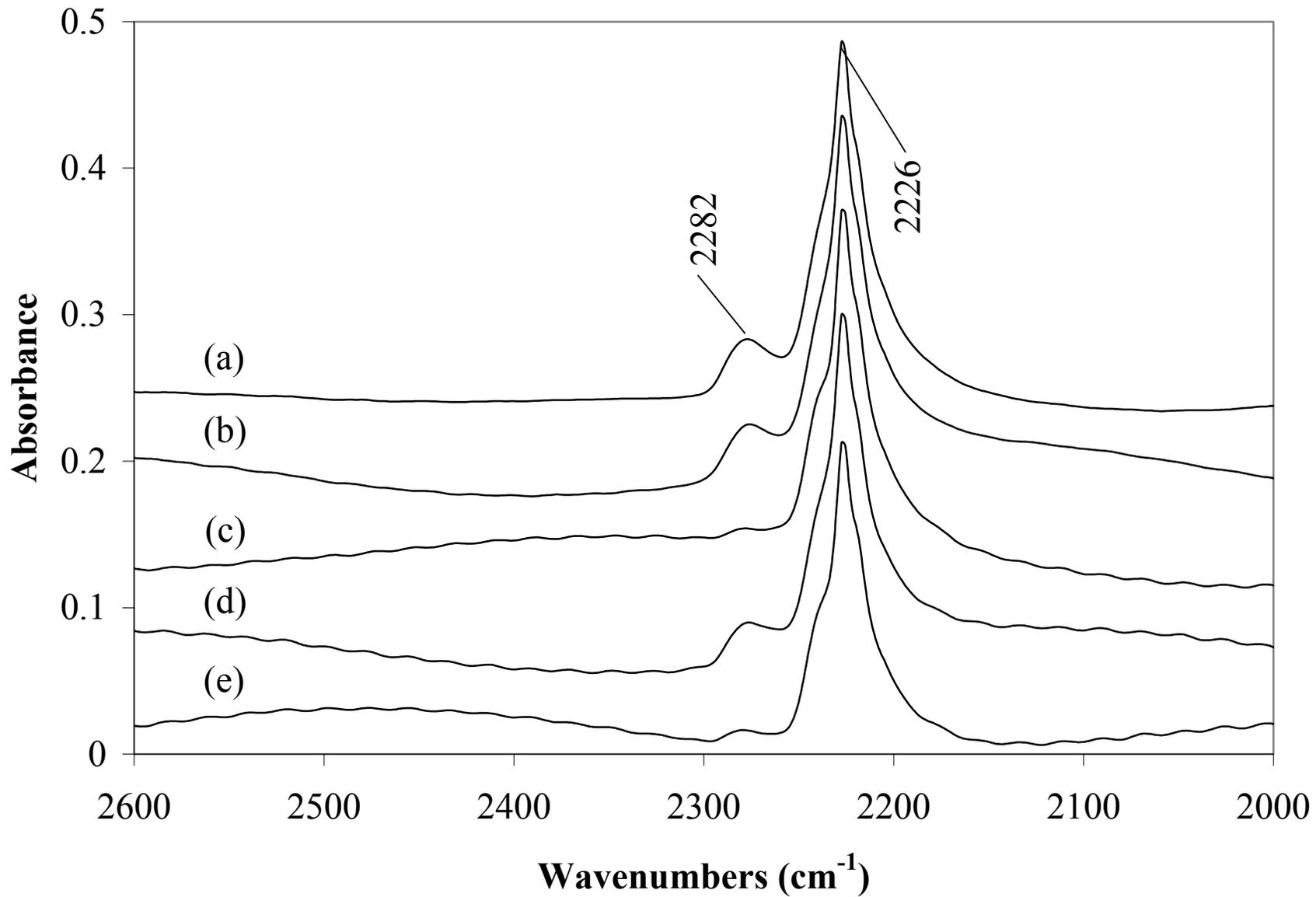
Fig. 5
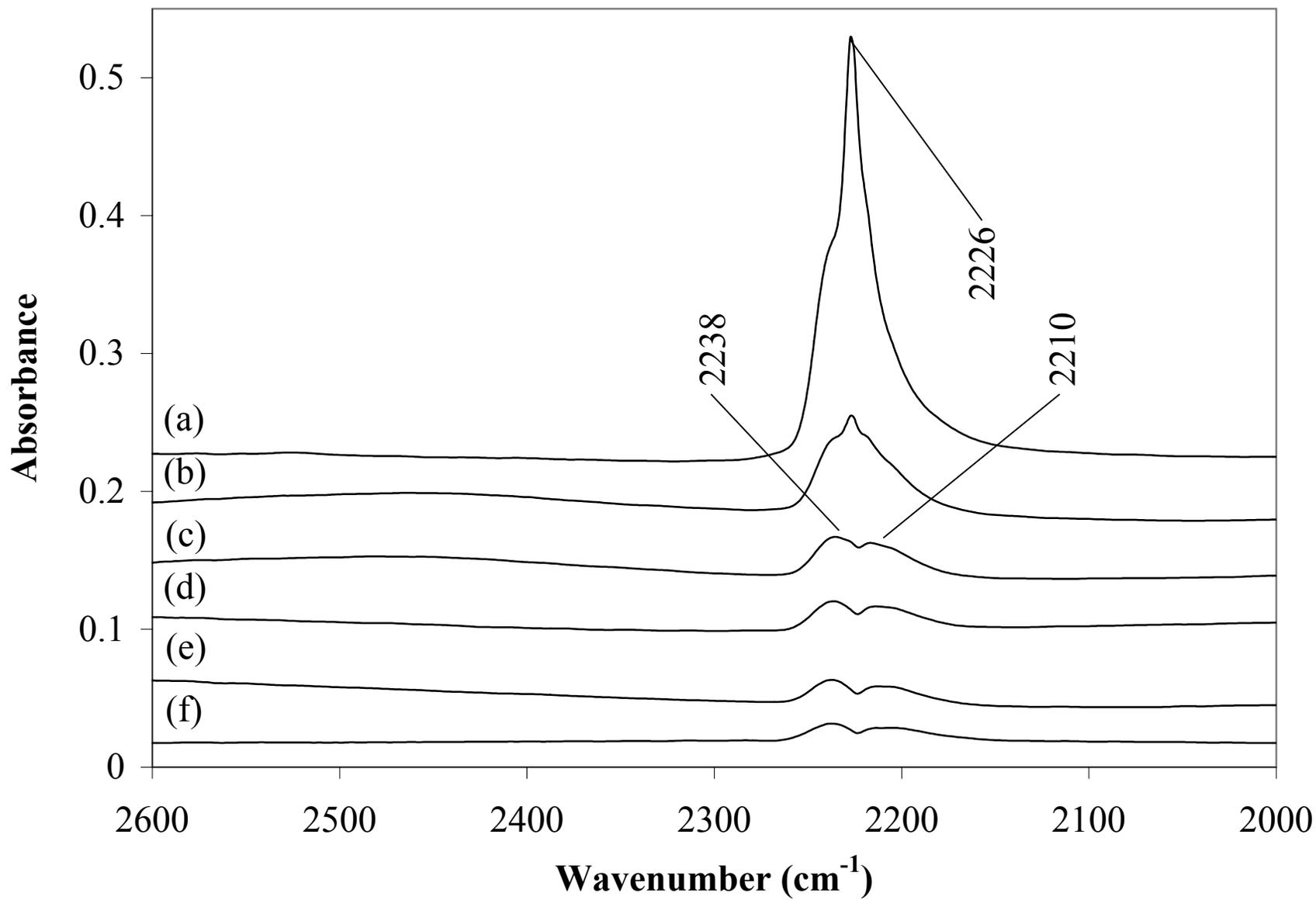
Fig. 6

Fig. 7

Fig. 8

Fig. 9

Fig. 10